

A. BEYERTT 
D. NICKEL
A. GIESEN

Femtosecond thin-disk Yb:KYW regenerative amplifier

Universität Stuttgart, Institut für Strahlwerkzeuge, Pfaffenwaldring 43, 70569 Stuttgart, Germany

Received: 20 December 2004 /
Revised version: 23 February 2005 /
Published online: 13 April 2005 • © Springer-Verlag 2005

ABSTRACT We report a compact thin-disk Yb:KYW regenerative amplifier system. Two different concepts are investigated to obtain either subpicosecond pulses with up to 160 μJ or a pulse energy of 20 μJ with a pulse width of about 300 fs. The first concept uses intra-cavity group-velocity dispersion compensation with Gires–Tournois interferometer mirrors to avoid pulse stretching during amplification. The onset of nonlinear effects in this concept inhibits the generation of shorter pulse durations at this energy level. Shorter pulses can be achieved with the second concept, which is based on dispersive pulse stretching during amplification and uses pulse compression after amplification with a grating compressor. Repetition rates up to 45 kHz are demonstrated.

PACS 42.65.Re; 42.60.Da; 42.55.Xi

1 Introduction

Compact sources of ultra-short laser pulses with energies up to several 100 μJ are of interest for many applications, such as micromachining and medical surgery where extremely precise ablation of all kinds of materials is required. For applications in dentistry, for example, subpicosecond pulses in the 100- μJ energy level are preferable [1] while other applications require pulse energies of several microjoules with shorter pulse widths.

The general problem encountered when amplifying ultra-short pulses to these energy levels is that unacceptably high peak intensities are easily reached in optical components. High peak intensities cause nonlinear pulse-shape distortions and optically induced damage of the components. One method of reducing the peak power of ultra-short pulses in an optical amplifier is temporal stretching of the pulses to several 100 ps prior to the amplification and recompressing afterwards. This technique is called chirped pulse amplification (CPA) [2]. A disadvantage of these systems is their relatively high complexity.

A different approach to lower the peak intensities in the amplifier is to enlarge the beam cross-sectional area in all critical optical components. This can be achieved in the laser-

active material by using the thin-disk laser concept [3] for the regenerative amplifier. Combined with a suitable resonator design it eliminates the need for the CPA technique for conditions with moderate power densities as presented in this paper.

Today, commercially available ultra-short-pulse laser systems with high energies are mainly based on Ti:sapphire amplifiers. The CPA technique is essential in these systems. Repetition rates at high pulse energies are limited to several kHz. Ti:sapphire lasers require green pump light and cannot be pumped by diodes directly. Thus, these commercial systems are still bulky, maintenance demanding, and very expensive.


In recent years the demand for compact and robust turn-key ultra-short pulse sources has initiated a new generation of ultra-short lasers based on optical fibers and thin disks as gain media. Fiber-based chirped pulse amplification systems producing femtosecond pulses with energies exceeding 1 mJ with average powers of about 10 W were demonstrated [4]. With a thin-disk regenerative amplifier, pulse durations of 750 fs and pulse energies of 100 μJ with repetition rates up to 45 kHz were demonstrated [5]. Both systems have the potential to become commercial turn-key systems.

We report two Yb:KYW thin-disk regenerative amplifiers based on different concepts. The first is an Yb:KYW thin-disk amplifier without CPA [5, 6], where Gires–Tournois interferometer (GTI) mirrors [7] are implemented in the amplifier cavity for group-velocity dispersion (GVD) compensation. The second is an Yb:KYW regenerative amplifier without stretcher and without GTI mirrors, but with a grating compressor [8] for compressing the pulses after amplification. The first concept is suitable for the amplification of subpicosecond pulses to energy levels of several 100 μJ . The advantage of this concept is its simple and compact set-up. The second concept is more sophisticated and allows the amplification of shorter pulse widths.

2 Experimental set-up

The regenerative amplifier system consists of a seed laser, a beam telescope, a beam-separation unit, and the amplifier resonator, as shown in Fig. 1.

A diode-pumped Yb:glass laser oscillator, which is passively mode locked using a semiconductor saturable absorber mirror [9], is employed as seed laser. It is protected against feedback by an optical isolator. The mode of the seed laser beam is matched to the amplifier resonator using a telescope.

 Fax: +49-711-6856842, E-mail: angelika.beyertt@ifsw.uni-stuttgart.de

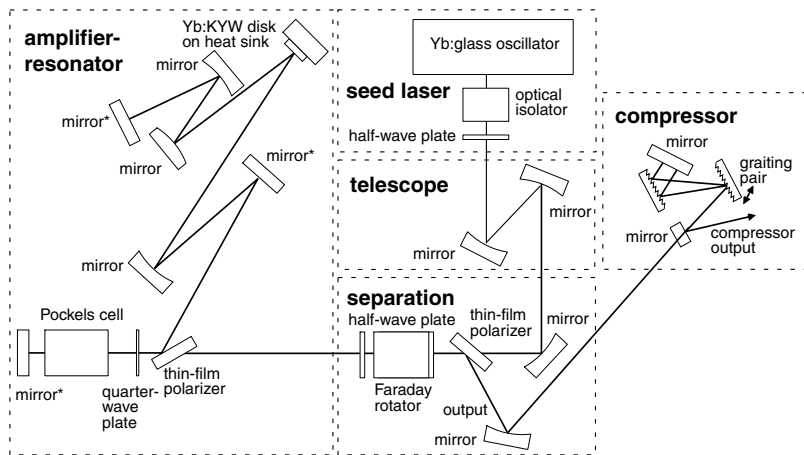


FIGURE 1 Scheme of the experimental set-up. In the case of intra-cavity dispersion compensation, resonator mirrors marked with an asterisk (*) are replaced by GTIs and the compressor is not used

A thin-film polarizer in combination with a Faraday rotator and a half-wave plate are used to separate the amplified pulses from the seed pulses.

The amplifier resonator is designed for TEM₀₀ operation. A BBO Pockels cell and a thin-film polarizer are used for injection and ejection. The high voltage, which is applied to the 20-mm-long BBO crystal in the Pockels cell, is switched by a fast solid-state switch. The repetition rate of the system is limited to 45 kHz by this switch.

When the quarter-wave voltage is applied to the Pockels cell, one seed pulse is trapped in the resonator and is amplified in the Yb:KYW thin disk during several round trips until the Pockels cell voltage is switched off again. The 100- μm -thick, wedged, 10%-doped Yb:KYW *b*-cut crystal is mounted with the HR-coated back side on a heat sink in a thin-disk laser head [10]. The disk is pumped through the AR-coated front side with a 60-W fiber-coupled diode laser at 981 nm. The thin-disk laser pump optics allows 16 pump beam passes through the disk. The pump spot diameter is 1.1 mm. Due to the weak gain, more than 100 resonator round trips are necessary for the desired amplification (total gain $G \approx 50$ dB).

With zero voltage applied to the Pockels cell the incoming seed pulse train circulates through the amplifier resonator only once; therefore, it is passing the gain medium twice. For a pump power of 60 W we measure a small-signal net gain of about 10% per round trip. When the quarter-wave voltage is applied to the Pockels cell, the pulse circulating in the resonator is trapped, whereas the incoming seed pulse train is rejected directly from the amplifier after passing the Pockels cell/quarter-wave plate combination. These rejected pulses and the pulses amplified in one round trip can be measured at the output of the regenerative amplifier and result in a constant background power level with high repetition rate. If this background is not tolerable for the application, a pulse picker selecting just one seed laser pulse for amplification has to be used.

The pulses are stretched during the amplification process mainly because of the positive GVD of the Pockels cell material combined with nonlinear effects. To compensate the positive GVD of the resonator two different concepts are applied. The first approach is to implement GTI mirrors in the resonator to compensate this GVD during the amplification [11]. The compensation has been optimized by testing differ-

ent combinations of several GTI mirrors with a GVD of about -100 , -500 , and -900 fs². The shortest pulses were observed using GTI mirrors with a total negative GVD of ≈ -1900 fs² per resonator round trip. But, since the applied GTI mirrors allow only discrete values of compensation, the GVD of the system could not be exactly compensated.

In the second approach, pulse stretching during amplification caused by the positive GVD is allowed, and the pulses are compressed after the amplification using diffraction gratings. At a first glance, the second approach is very similar to traditional chirped pulse amplification schemes, but we do not need a dedicated stretcher stage before amplification. Pulse stretching is simply based upon dispersive pulse stretching due to the optical components inside the amplifier cavity. So, we need much less dispersion in the compressor and consequently can use gratings with lower groove density that results in a strongly relaxed alignment tolerance, thus avoiding one of the problems of CPA systems. The concept of intra-cavity stretching is known, particularly for Ti:sapphire systems, where the dispersion of standard intra-cavity components is sufficient to avoid nonlinear effects [12]. In our set-up a double-passed parallel grating pair was placed in the collimated amplifier output beam. The gold-coated replica gratings (1000-nm blaze wavelength) have a groove density of 600 grooves/mm. The gratings are aligned near the Littrow angle with an angle of incidence of 10°, and are separated by about 100 mm along the direction perpendicular to both faces. The transmission efficiency of the compressor stage is about 70%.

3 Experimental results

3.1 Regenerative amplifier with intra-cavity GVD compensation by using GTIs

For these experiments we used an Yb:glass seed laser oscillator running at 39-MHz repetition rate, and producing nearly bandwidth-limited pulses. The wavelength is tunable from 1025 to 1050 nm, and the pulse energy is about 1 nJ. The pulses are as short as 430 fs at a wavelength of 1030 nm, and at 1026 nm the pulse width increases to 670 fs (see Fig. 2). The seed wavelength has a significant influence on the amplification. The emission spectrum of Yb:KYW [13] shows its maximum at 1025 nm for a polarization parallel to

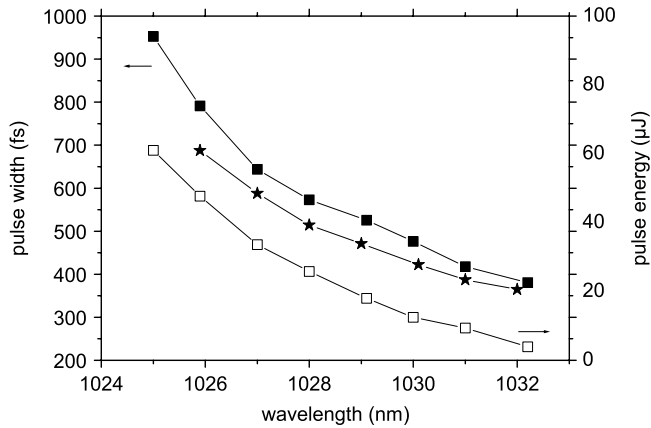


FIGURE 2 Influence of the seed laser wavelength at 90 resonator round trips on the pulse duration (closed symbols) and pulse energy (open symbols). The corresponding seed laser pulse widths are shown as stars

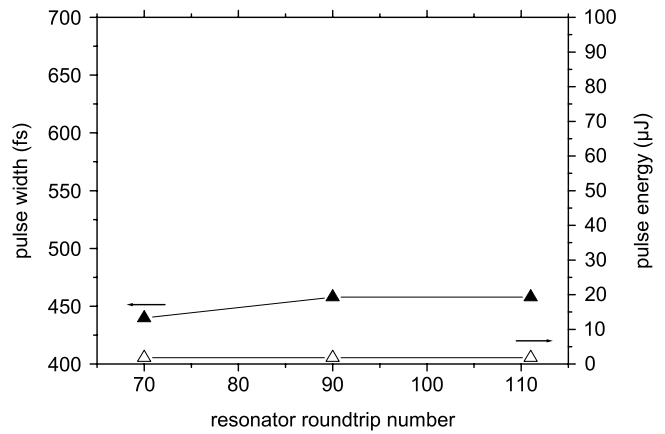


FIGURE 4 Pulse duration (closed symbols) and pulse energy (open symbols) of the amplified pulses as functions of the resonator round trip number. The pump power was adjusted for low pulse energy

the *a* axis of the crystal. This decreases the energy of the amplified pulses as the seed laser is tuned from 1025 nm to longer wavelengths with the same resonator round trip number, as can be seen in our experiments. Figure 2 shows the influence of the seed laser wavelength on the pulse energy and also on the pulse duration of the amplified pulses. To find a compromise between high amplification on one hand and short pulse duration on the other hand, the seed wavelength was set to 1030 nm for the presented experiments.

The energy and the duration of the amplified pulses are shown in Figs. 3 and 4 as functions of the number of resonator round trips. The experiments have been performed at 10-kHz repetition rate. The results in Fig. 3 have been achieved with a maximum pump power of 60 W. For the measurements shown in Fig. 4, the pump power was adjusted to achieve the same low pulse energy in the 2-μJ range for different resonator round trip numbers. The pulse widths (FWHM) were determined from autocorrelation traces of the amplified pulses assuming a sech^2 pulse shape. At maximum pump power and 111 resonator round trips the pulse energy was about 93 μJ and the pulse width 625 fs. The resonator round trip number was limited to 111 because of the onset of severe nonlinear pulse

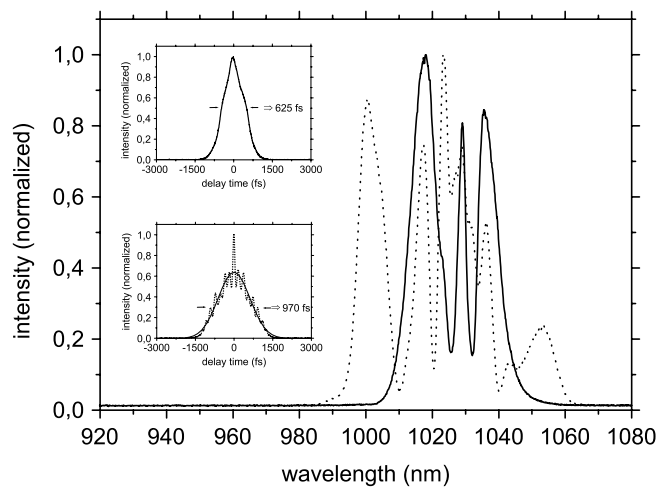


FIGURE 5 Spectra of amplified pulses with 93-μJ pulse energy using seed pulse width of 460 fs (solid line) and 100-μJ pulse energy using seed pulse width of 280 fs (dotted line). Upper inset: autocorrelation traces of amplified pulses with 93 μJ. Lower inset: autocorrelation traces with fit curve of amplified pulses with 100 μJ

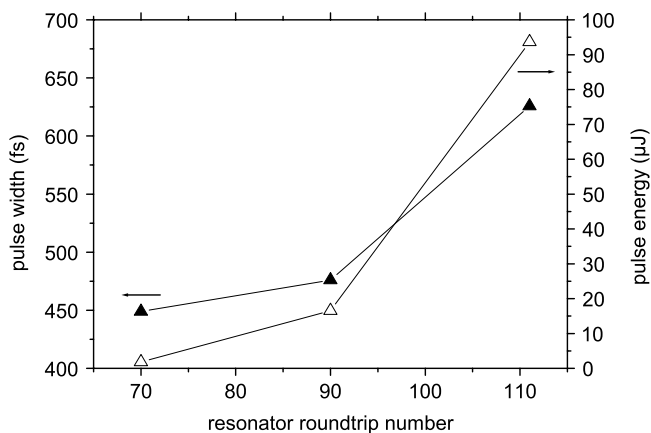


FIGURE 3 Pulse duration (closed symbols) and pulse energy (open symbols) of the amplified pulses as functions of the resonator round trip number. Maximum pump power was used

distortions, as can be seen from the optical pulse spectra and autocorrelation traces at higher pulse energies (Fig. 5).

In the case of the low pulse energy, the pulse duration was measured to be 450 fs for 70 resonator round trips, increasing slightly with the number of resonator round trips. The duration of the seed pulses was 420 fs. The *B*-integral [14] taking pulse energies, pulse width, resonator round trip number, and the nonlinear refractive index for BBO of $2.9 \times 10^{-16} \text{ cm}^2/\text{W}$ [15] and for Yb:KYW of $8.7 \times 10^{-16} \text{ cm}^2/\text{W}$ [16] into account is estimated to be $B \leq 0.09\pi$. The nonlinearity is dominated by the Pockels cell material with negligible contribution from the thin disk. The pulse lengthening is caused by a combination of the residual GVD in the system, which is not exactly compensated by the GTIs, and nonlinear effects.

Experiments with shorter seed pulses of 260 fs (Yb:glass laser oscillator, 50 MHz, 2.5 nJ) in this set-up led to an even faster onset of nonlinearities for all energies. Figure 5 gives a comparison of the spectra of the amplified pulses with the corresponding autocorrelation traces using seed pulses of 260

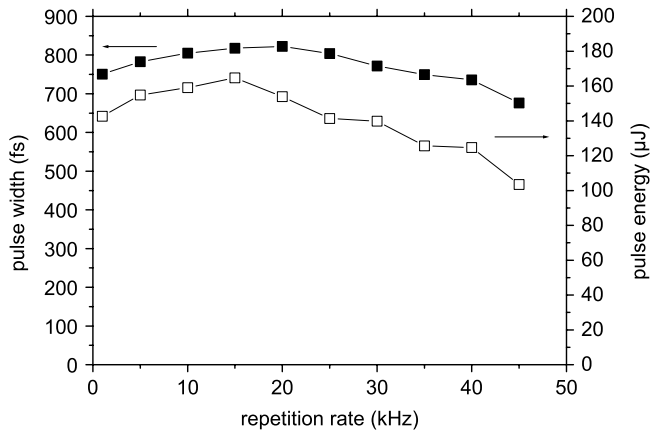


FIGURE 6 Pulse duration (closed symbols) and pulse energy (open symbols) of the amplified pulses as functions of the repetition rate of the amplifier

and 420 fs. Both spectra have been recorded with similar pulse energies (100 and 93 μJ) and similar numbers of resonator round trips (108 and 111). The spectrum, as well as the autocorrelation traces, shows much more distortion in the case of the shorter seed pulses (pulse width obtained from a fit to the autocorrelation trace). The pulse width increases to 970 fs as compared to 625 fs for the longer seed pulses. The B -integral is estimated to be $B \gg \pi$ in both cases. The nonlinear effects set a limit for the shortest achievable pulse width. It is impossible to increase the pulse energy much beyond the 200-μJ level in the subpicosecond time domain with the current operating parameters. Even limiting the pulse energies to several microjoules does not allow us to demonstrate a pulse width of about 300 fs in this set-up.

Finally, experiments with different repetition rates up to 45 kHz and a slightly higher negative total GVD of the GTIs of $\approx -2000 \text{ fs}^2$ per resonator round trip were performed. The pulse energy and the pulse duration of the amplified pulses in dependence on the repetition rate are presented in Fig. 6. For these measurement 125 resonator round trips were used. At 10 kHz a pulse energy of 160 μJ was obtained with a pulse width below 900 fs. At 45 kHz the pulse energy decreases to 100 μJ with a pulse width of 670 fs.

The beam quality measured according to ISO 11146 [17] using a 12-bit CCD camera is $M^2 < 1.3$.

3.2 Regenerative amplifier with grating compressor

For applications demanding shorter pulse widths the second concept is more suitable. We used an Yb:glass laser with a repetition rate of 50 MHz, a fixed wavelength of 1030 nm, a pulse energy of about 2.5 nJ, and bandwidth-limited pulses with a pulse width of 290 fs as seed laser.

All GTI mirrors were replaced by standard highly dielectric resonator mirrors in this set-up, resulting in a positive net dispersion of about 1900 fs^2 . The seed pulses were amplified during 83 resonator round trips with maximum pump power, leading to an output pulse energy of 28 μJ (before compression). The experiments were performed at 10-kHz repetition rate. The seed pulse width was 290 fs, whereas the amplified pulses show a pulse width of 1.75 ps. Because of the spectral broadening in the amplifier resonator the pulse width

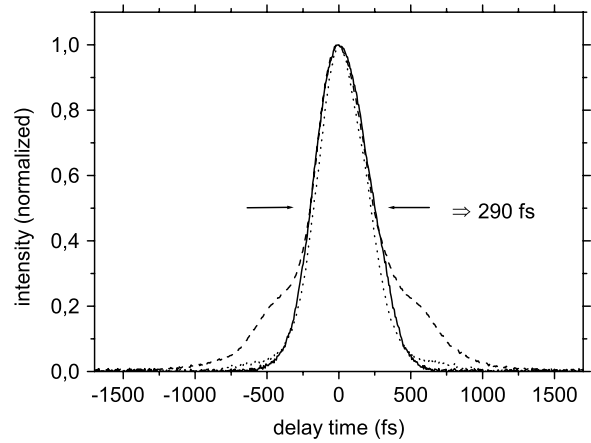


FIGURE 7 Intensity autocorrelation traces of the seed laser pulses (solid line), compressed pulses at a pulse energy of 28 μJ (dotted line), and compressed pulses at a pulse energy of 150 μJ (dashed line)

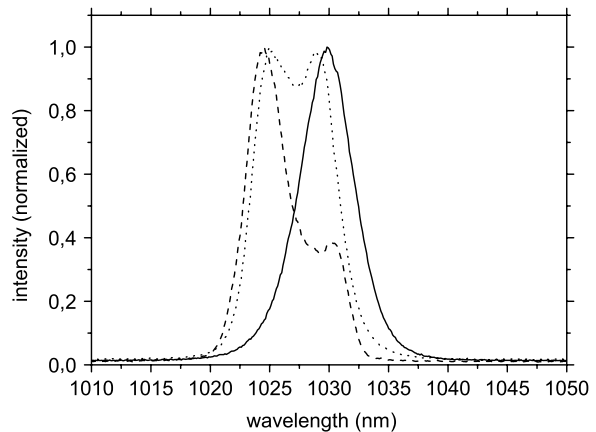


FIGURE 8 Pulse spectra of seed laser (solid line) and amplified pulses at a pulse energy of 28 μJ (dotted line) and 150 μJ (dashed line)

after passing the compressor stage (270 fs) is slightly shorter than the seed pulse width. The autocorrelation traces are presented in Fig. 7. The spectra, which can be seen in Fig. 8, are broadened due to the spectral shape of the gain and shifted towards the emission spectrum maximum of Yb:KYW. The B -integral was estimated to be $B \leq 0.16\pi$ (for a pulse energy of 28 μJ). After compression, the autocorrelation trace of the pulses shows a small pedestal mainly due uncompressed higher-order dispersion.

Additionally, we studied the compression at a much higher pulse energy of 150 μJ (before compression) using 100 resonator round trips. The separation of the gratings had to be adapted to the number of resonator round trips to be about 120 mm, as it depends on the material path length passed during amplification. The autocorrelation traces of the pulses can also be seen in Fig. 7. The uncompressed pulses have a width of 2.07 ps. The compressed pulses have the same FWHM pulse width as the seed pulses, but possess an enlarged pedestal due to uncompressed higher-order dispersion, and the B -integral of $B \leq 0.58\pi$ suggests the onset of nonlinear effects. Comparing the spectrum of the pulses using the compressor concept (Fig. 8) with the GVD compensation scheme using GTIs (Fig. 5) shows that the spectra become less

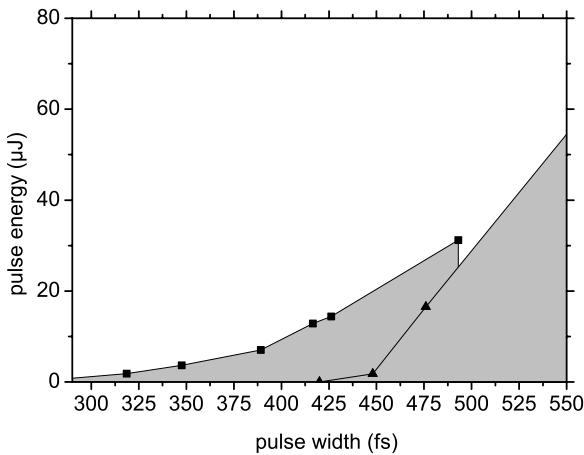


FIGURE 9 Achievable pulse energies and pulse widths with B -integral $B \leq \pi$ for the intra-cavity GVD compensation concept (dark-grey area). Measured values for a seed laser pulse width of 260 fs as squares and for a seed laser pulse width of 420 fs as triangles (curve extrapolated to measured higher values)

distorted in the compressor concept where the peak intensities are reduced.

The beam quality in this set-up is also measured to be $M^2 < 1.3$, i.e. the beam quality does not degrade by the use of the grating compressor.

4 Comparison of the two concepts

To compare both systems the generally accepted criterion for high-power laser systems that the cumulative B -integral should be kept below $B \approx \pi$ to avoid serious nonlinear effects [13] is taken into account. In Fig. 9 the achieved energy versus the pulse width is shown for the intra-cavity GVD compensation with seed laser pulse widths of 260 and 420 fs as described in Sect. 3.1, with a B -integral $B \leq \pi$. In this case the spectra show no major distortion. Only pulses with energies and pulse widths in the dark gray pictured area have been realized in this set-up with a B -integral $B \leq \pi$. Longer seed pulse widths allow higher energies, but at longer pulse widths. With the concept using the grating compressor, up to 150 μJ with a pulse width of about 290 fs has been demonstrated with a B -integral of $B \leq 0.58\pi$. Larger pulse widths can easily be achieved by reducing the compression ratio. Thus, the compressor concepts permits application over a greater range of pulse energies and pulse widths with a B -integral of $B \leq \pi$, at the price of a more sophisticated system.

To expand the operational area with a B -integral $B \leq \pi$ for the intra-cavity GVD compensation concept, several steps can be taken. These steps hold as well to improve the compressor concept.

To reduce the number of resonator round trips, and therefore the nonlinear interaction length, the small-signal gain per resonator round trip can be increased by, for example, choosing a resonator design that allows four bounces on the Yb:KYW thin disk per resonator round trip [18]. To further enhance the small-signal gain a seed laser wavelength of 1025 nm, which is better adapted to the amplifying medium, can be used.

To minimize the nonlinear effects, the beam diameter in the Pockels cell crystal can be enlarged and the length of the Pockels cell crystal can be reduced. This step is limited by the availability of high-voltage switches, as the necessary quarter-wave voltage increases by enlarging the crystal aperture and reducing the crystal length.

With these steps, pulse energies up to 200 μJ with a pulse width of 500 fs seem feasible with a B -integral $B \leq \pi$ for the intra-cavity GVD compensation concept.

5 Conclusion

We have demonstrated a compact all-solid-state 100-μJ-level Yb:KYW thin-disk regenerative amplifier system to provide ultra-short pulses. Pulses with durations below 1 ps and energies in the 100-μJ range with repetition rates of up to 45 kHz were realized in a very compact, easily adjustable amplifier system including intra-cavity GVD compensation by GTI mirrors. Nonlinear effects in this set-up constrain the pulse width even at low pulse energies. For applications like material processing, where high energy densities and focusability are of major interest, higher B -values, resulting in modulated spectra, can be accepted as long as the beam quality is as good as demonstrated ($M^2 < 1.3$). In this case the intra-cavity GVD compensation concept may be favorable due to the simpler set-up.

To achieve shorter pulse widths of about 300 fs with pulse energies up to the hundred-microjoule energy level, a grating compressor was used. This compressor set-up is still simple and less susceptible to misalignment than the usual CPA systems, as we use a lower groove density and no stretcher is needed.

ACKNOWLEDGEMENTS We are grateful to A. Kasenbacher (Traunstein, Germany), the Fachhochschule Mannheim MABEL (Mannheim Biomedical Engineering Laboratories, Germany), the BMBF (German Ministry for Education and Research), and Jenoptik LOS GmbH (Jena, Germany) who financially supported this research.

REFERENCES

- 1 J. Serbin, T. Bauer, C. Fallnich, A. Kasenbacher, W.H. Arnold, Appl. Surf. Sci. **197–198**, 737 (2002)
- 2 D. Strickland, G. Mourou, Opt. Commun. **56**, 219 (1985)
- 3 A. Giesen, H. Hügel, A. Voss, K. Wittig, U. Brauch, H. Opower, Appl. Phys. B **58**, 365 (1994)
- 4 A. Galvanauskas, IEEE J. Sel. Top. Quantum Electron. **7**, 504 (2001)
- 5 A. Beyertt, D. Müller, D. Nickel, A. Giesen, in *OSA Trends in Optics and Photonics*, ed. by G.J. Quarles. Advanced Solid-State Photonics, vol. 94 (Optical Society of America, Washington, DC, 2004), presentation no. WA5
- 6 A. Beyertt, D. Müller, D. Nickel, A. Giesen, in *OSA Trends in Optics and Photonics*, ed. by J.J. Zayhowski. Advanced Solid-State Photonics, vol. 83 (Optical Society of America, Washington, DC, 2003), p. 407
- 7 F. Gires, P. Tournois, C. R. Acad. Sci. **258**, 6112 (1964)
- 8 E.B. Treacy, IEEE J. Quantum Electron. **QE-5**, 454 (1969)
- 9 D. Kopf, F.X. Kärtner, U. Keller, K.J. Weingarten, Opt. Lett. **20**, 1169 (1995)
- 10 S. Erhard, K. Contag, I. Johannsen, M. Karszewski, T. Rupp, C. Stewen, A. Giesen, in *OSA Trends in Optics and Photonics*, ed. by M.M. Fejer, H. Injeyan, U. Keller. Advanced Solid-State Lasers, vol. 26 (Optical Society of America, Washington, DC, 1999), p. 38
- 11 J. Heppner, J. Kuhl, Appl. Phys. Lett. **47**, 453 (1985)
- 12 T.B. Norris, Opt. Lett. **17**, 1009 (1992)

- 13 N.V. Kuleshov, A.A. Lagatsky, V.G. Shcherbitsky, V.P. Mikhailov, E. Heumann, T. Jensen, A. Diening, G. Huber, *Appl. Phys. B* **64**, 409 (1997)
- 14 A.E. Siegman, *Lasers* (University Science Books, Mill Valley, CA, 1986), p. 385
- 15 R. DeSalvo, A.A. Said, D.J. Hagan, E.W. Van Stryland, M. Sheik-Bahae, *IEEE J. Quantum Electron.* **32**, 1324 (1996)
- 16 K.V. Yumashev, N.N. Posnov, P.V. Prokoshin, V.L. Kalashnikov, F. Mejid, I.G. Poloyko, V.P. Mikailov, V.P. Kozich, *Opt. Quantum Electron.* **32**, 43 (2000)
- 17 ISO 11146, Test methods for laser-beam parameters: beam width, divergence angle, and beam-propagation factor
- 18 F. Butze, M. Larionov, K. Schuhmann, C. Stolzenburg, A. Giesen, in *OSA Trends in Optics and Photonics*, ed. by G.J. Quarles. *Advanced Solid-State Photonics*, vol. 94 (Optical Society of America, Washington, DC, 2004), presentation no. WA 4